To be published in Applied Optics:

Title:	Optical properties of apple skin and flesh in the wavelength range from 350 to 2200 nm
Authors:	Wouter Saeys, Maria Velazco-Roa, Suresh Thennadil, Bart. Nicolai, and Herman Ramon
Accepted:	3 January 2008
Posted:	9 January 2008
Doc. ID:	87102

Optical properties of apple skin and flesh in the wavelength range from 350 to 2200 nm

Wouter Saeys,[1,*] Maria A. Velazco-Roa,[2] Suresh N. Thennadil[2], Herman Ramon[1], and Bart M. Nicolaï[1]

[1]*Division of Mechatronics Biostatistics and Sensors, Department of Biosystems, Katholieke Universiteit Leuven, Kasteelpark Arenberg 30, B-3001 Heverlee, Belgium*

[2]*Merz Court, Chemical Engineering and Advanced Materials, University of Newcastle upon Tyne, Newcastle upon Tyne, NE1 7RU, United Kingdom*

[*]*Corresponding author: wouter.saeys@biw.kuleuven.be*

Optical measurement of fruit quality is challenging due to the presence of a skin around the fruit flesh and the multiple scattering by the structured tissues. To gain insight in the light-tissue interaction, the optical properties of apple skin and flesh tissue are estimated in the 350-2200 nm range for three cultivars. For this purpose, single integrating sphere measurements are combined with inverse adding-doubling. The observed absorption coefficient spectra are dominated by water in the NIR and by pigments and chlorophyll in the visible region, whose concentrations are much higher in skin tissue. The scattering coefficient spectra show the monotonic decrease with increasing wavelength typical for biological tissues with skin tissue being about 3 times more scattering than flesh tissue. Comparison to the values from time resolved spectroscopy reported in literature showed

comparable profiles for the optical properties, but overestimation of the absorption coefficient values, due to light losses.

OCIS codes: 290.7050, 300.1030, 290.0290, 290.4210, 300.6340, 300.6550.

1. Introduction

During the last decade the potential of Vis/NIR spectroscopy for the non-destructive measurement of the physical and chemical quality parameters of fruit has been investigated by many research groups worldwide [1]. Since apples are the most economically important fruit after bananas worldwide, they have been the subject of a large number of these studies [1-8]. While absorption in the Vis/NIR range is related to some important chemical quality attributes such as the total sugar content, scattering is related to the microstructure of the tissue, and, hence, the macroscopic texture properties of the fruit [9]. The relation for estimating the aforementioned quality attributes from the Vis/NIR reflectance, interactance or transmittance spectrum of the fruit is typically established based on a large calibration dataset using chemometrical techniques. As the spectral measurements can be carried out in a noninvasive way, they potentially could be used advantageously to grade fruit based on its organoleptic quality attributes rather than on visual appearance as is now almost always the case.

The industry has now adopted this technology, and many manufacturers of on-line grading lines have implemented Vis/NIR systems to measure quality attributes of a variety of fruit. However, their accuracy and robustness is often limited. This is partly due to the fact that, although we are mostly interested in the properties of the flesh, the radiation has to travel through the skin and will, therefore, be considerably influenced by the skin properties. Also, both the skin and flesh are structured tissues with many cell wall interfaces and suspended particles, which cause

multiple scattering of the light passing through them. To obtain better non-destructive measurements of the relevant properties it is, therefore, essential to have a better understanding of the interaction of the radiation with the fruit tissue

Cubeddu et al. [10] used time-resolved reflectance spectroscopy (TRS) to measure the absorption and transport scattering coefficients μ_a and μ_s' for 3 apple varieties in the 650 to 1000 nm range, while Nicolaï et al. [11] estimated those for Conference pears in the 875-1030 nm range. However, in both studies the lumped bulk properties for skin and flesh were estimated together, while there obviously is a clear difference in the optical properties of both layers, since we can visually discriminate them. It would, therefore, be more appropriate to consider the skin and peel as two distinct layers when investigating the interaction of radiation with fruit [12]. Moreover, the available optical properties [10] are limited to the 650-1000 nm range, while most applications consider a broader spectrum [2-8]. Thus, the objective of this study was to obtain the optical properties of both apple skin and flesh in the wavelength range from 350 to 2200 nm.

Optical properties measurement over such a broad wavelength range is currently not possible by means of time-resolved reflectance spectroscopy (TRS). Therefore, we will apply a methodology based on continuous-wave reflectance spectroscopy (cw) using an integrating sphere setup and inversion procedure, inspired by the one Troy and Thennadil [13] successfully applied to measure both the absorption coefficient μ_a and the transport scattering coefficient μ_s' of human skin in the near infrared range from 1000 to 2200 nm. However, since double integrating sphere setups are not commonly available and represent a serious extra cost, we will apply a methodology using a standard spectrophotometer setup equipped with an integrating sphere module [14].

First, the possibility to estimate the absorption coefficient μ_a and the transport scattering coefficient μ_s' for a fixed value of the anisotropy coefficient g based on sequential measurements of the total transmittance T_t and the total reflectance R_t will be investigated. Secondly, the feasibility to estimate the wavelength dependent anisotropy coefficient g as well by means of a collimated transmittance T_c measurement will be investigated. This methodology incorporates the major assumption that the sequential *in vitro* measurements on apple tissue samples are reasonably representative for the *in vivo* tissues. Finally, by measuring different cultivars, different shelf life and different spots on each apple the average bulk optical properties and the variation around these will be estimated.

2. Materials and Methods

A. System setup

All spectral measurements are performed in the 350 to 2200 nm range using a scanning monochromator spectrophotometer (Cary 5000, Varian Inc., Palo Alto, CA). In the range from 350 to 800 nm an average integration time of 0.4 s, a signal band width of 4.0 nm and a wavelength interval of 1.0 nm are applied for the photomultiplier tube (PMT) detector. The Peltier (TE) cooled PbS detector for the range from 800 to 2200 nm is operated at an average integration time of 0.4 s, a signal band width of 8.0 nm and a wavelength interval of 4.0 nm. This results in 801 discrete observations per measured spectrum. The collimated transmittance T_c is measured with the instrument's standard configuration where the tissue sample is placed in the line between the exit slit of the monochromator and the entrance slit of the detector. For the total reflectance R_t and total transmittance T_t measurements an external diffuse reflectance accessory (External DRA-2500, Varian Inc., Palo Alto, CA) is mounted. This external Diffuse Reflectance

accessory consists of a 150 mm diameter integrating sphere which has a port-to-sphere area ratio of less than 10%. The sphere is coated with 4 mm thick and 1 g/cm^3 dense Polytetrafluoroethylene (PTFE) and has inbuilt high performance photomultiplier tube (PMT) and Lead Sulfide (PbS) detectors. A schematic representation of the different measurement configurations is shown in Figure 1. In case of a total transmittance measurement T_t, the sample is placed at the entrance port of the sphere, while the exit port is blocked with a PTFE reflectance standard. In this way, all light transmitted (both collimated and diffuse) through the sample is collected by the detector. For a total reflectance measurement, the sample is placed at the exit port of the sphere, so that all light reflected by the sample is collected in the sphere and directed towards the detector. To obtain the same diameter for the illumination spot different focussing lenses are used for the reflectance and transmittance measurements. Each of the measured intensity spectra is divided by the intensity spectrum measured for a calibrated reference to express the reflectance and transmittance as relative fractions ranging from 0 to 1.

B. Data Analysis

The optical properties are obtained from the measured total reflectance R_t, the total transmittance T_t and the collimated transmittance T_c by means of an inverse adding-doubling program running under Matlab 6.5 (The Mathworks Inc., Natick, MA). The core of this program consists of a numerical solution to the one speed radiative transport equation (RTE), which describes light propagation at steady state in a scattering medium, by means of the adding-doubling approach with a Henyey-Greenstein phase function which incorporates the effects of glass slabs surrounding the sample [14, 15]. Since this numerical solution of the radiative transport equation calculates the total reflectance R_t and the total transmittance T_t for a given set of optical properties, it has been incorporated in a constrained optimization scheme for nonlinear

multivariable functions ('fmincon' function of the Matlab® optimization toolbox) to find a set of feasible optical properties for which the calculated reflectance and transmittance values match the measured ones.

This approach has been successfully applied in the past for estimation of the absorption coefficient μ_a and the transport scattering coefficient μ_s' of human tissue based on the measured total transmittance T_t and the total reflectance R_t when both the anisotropy coefficient g and the refractive index n of the sample are given [13]. In human tissue optics, the anisotropy coefficient g has been shown to vary between 0.8-0.9 and some sensitivity analysis has shown that μ_a and μ_s' estimation is not very sensitive to the value of g in this region. For apples we do not know the range of values g can take. Therefore, the inversion program has been extended to estimate the anisotropy factor g as well by including the collimated transmittance T_c.

It is known that, while in principle the three optical properties (μ_a, μ_s and g) can be obtained from measurements of the collimated transmittance T_c, total transmittance T_t and the total reflectance R_t, the estimates can be prone to a lot of error in the case of light losses from the integrating sphere setup and due to the high correlation between T_c and T_t [16]. Although it would be better to have an independent measurement for the estimation of g, this is not easily achievable using standard spectroscopic equipment. Therefore, we will investigate the feasibility of constrained optimization to obtain good estimates for the optical properties based on the three correlated measurements.

The constrained optimization makes it possible to ensure that the estimated values for the albedo ($\mu_s/(\mu_a+\mu_s)$) and the anisotropy coefficient g are kept respectively between 0 and 1, and -1 and 1. In this way, it is avoided that the iterative optimization becomes unstable by reaching unrealistic values for the model parameters. Constrained optimization demands an initial guess

from which the iteration can be started. This value should be chosen wisely to minimize the number of iterations needed to find the optimum and to avoid ending up in a local minimum. Since the optical properties are expected to be continuous functions of the wavelength, it is chosen to use the estimated value of the previous wavelength as the initial guess for the next wavelength. In this way, the number of iterations (and thus also the computation time) is decreased considerably and smooth estimates are obtained. Around the water peaks, the error on the estimated values is, however, rather high due to the low collimated and total transmission values. Therefore, it is chosen not to update the initial guess with the newly estimated value when the measured collimated transmittance is below 0.01%.

C. Validation Procedure

There are two parts to validation of the presented approach. The first part consists of quantifying the estimation error on the absorption coefficient μ_a and the scattering coefficient μ_s for a fixed value of the anisotropy coefficient g based on measurements with the integrating sphere set-up. This mirrors the situation where the value of g is either assumed using prior knowledge of the particulate system or through independent estimation of g from either measurements or theoretical calculations. The second one lies in estimating how well we are able to estimate all three optical properties by using the three measurements (T_t, T_c and R_t).

For the first validation we will apply a procedure similar to the one described by Troy and Thennadil [13]. We use a model system consisting of a monodisperse suspension of polystyrene spheres of known diameter (0.45 μm) and concentration (0.15% by weight of solids), in water and compute μ_a, μ_s and g for this model system using Mie theory and the optical constants of water measured by Hale and Querry [17]. A sample of this model system was scanned in a 1 mm quartz glass cuvette in all three modes (T_t, R_t and T_c). The inverse adding-

doubling program is then used to estimate μ_a and μ_s in the range from 450 to 1800 nm based on the measured T_t and R_t values and 'known' values of g (i.e. computed using Mie theory for this sample). The estimated values are then compared to the ones obtained with Mie theory. It should be noted that, although the sample was scanned in the 350 to 2200 nm range, the validation is restricted to the 450 to 1800 nm range because we only had reasonable estimates for the refractive index values n and k required for using the Mie theory in this range.

Although it is known [16] that estimating g together with μ_a and μ_s using a double integrating sphere setup and inverse adding-doubling is prone to error, the possibility to estimate g together with μ_a and μ_s for the model system of polystyrene spheres by using the independently measured collimated transmittance T_c is investigated. By comparison of the obtained estimates for the absorption and scattering coefficients we also get insight in the impact this simultaneous estimation of the anisotropy factor has on the estimated scattering and absorption coefficients. In this way, we will try to get an idea of the reliability of this procedure for the estimation of the optical properties of apple tissue.

D. Experimental Procedure for Apple Tissue Measurement

The sample set consists of 42 apples of three different cultivars (Royal Gala, Granny Smith and Braeburn), which were purchased from a local store. For each cultivar the 14 apples were chosen from the same box to be as uniform as possible with respect to appearance, ripeness stage and shelflife. After purchase the apples were stored under room temperature until the time of measurement, which results in storage periods ranging from 1 to 21 days. On each of the 9 measurement days 1 or 2 apples of each cultivar were measured at two spots at opposite sides on the equator (most and least colored side). For each spot samples from the skin and flesh were cut by means of an industrial razor blade cutter and excess moisture was removed by means of paper

tissue. Caliper measurements (accuracy ±0.03 mm) were taken to provide an accurate measurement of tissue sample thickness and the sample was placed between two 1 mm glass slabs (ISO 8037/1 certified for *in vitro* diagnostic) to minimize drying and oxidation effects due to contact with air. In case of the skin samples, all flesh cells were scraped away by means of the razor blade. For each of these samples all three measurements (T_t, R_t and T_c) were performed. The order of the three measurements (T_t, R_t and T_c) and of the cultivars was randomized over the different measurement sessions to avoid systematic effects of the measurement order being transferred in the estimated optical properties. For the calculation of the Fresnel reflection at the sample-glass interfaces an average refractive index of 1.37, measured by means of a refractometer (Refracto 30Px, Mettler Toledo, UK), is used for both skin and flesh.

For each of the 168 samples (3 cultivars, 14 apples per cultivar, 2 spots per apple, skin and flesh tissue) the optical properties (μ_a, μ_s and g) are estimated based on the 3 measured spectra (T_t, R_t and T_c) by means of the extended inverse adding-doubling program. From the estimated g values an average value for both apple skin and flesh tissue is derived and the estimation of μ_a and μ_s is repeated for fixed g using the inverse adding-doubling approach. The average optical properties of apple skin and flesh and the variation around this average obtained with both approaches are then compared for each cultivar. The estimated values will also be shortly compared to the ones obtained by Cubeddu et al. [10] using Time Resolved Spectroscopy (TRS) in the 650-1000 nm range.

Note that optical properties of apple fruit may depend on many factors including season, orchard, cultivation method, harvest and storage time, even within one cultivar [3]. The fruit used in this experiment rather served as a vehicle to illustrate both the methodology as well as how optical

properties may vary between apples. The results should, therefore, not be considered as representative for the three different cultivars. Future research should focus on these aspects.

3. Results and Discussion

A. Validation of the Experimental Setup for Fixed Anisotropy Factor

The upper plot in Figure 2 shows the values for the absorption coefficient μ_a estimated by the inverse adding-doubling using the anisotropy factor g obtained from Mie theory and the values of μ_a calculated as the sum of the absorption coefficient of water and the absorption coefficient of the particles obtained from Mie theory. It can be seen that both curves have very good agreement over most of the wavelength range considered. However, the water peak is slightly underestimated by the inverse adding-doubling. This can probably be explained by the low transmission values in this region which reduce the signal to noise ratio and thus reduce the relative accuracy of the estimated values. The lower plot in Figure 2 shows the values of the scattering coefficient μ_s estimated from the measurements using the inverse adding-doubling program together with the values obtained from Mie theory. There is very good agreement between both profiles of the scattering coefficient with the increasing wavelength. However, a small peak can be observed around 1450 nm in the scattering coefficient estimated by the inverse adding-doubling. This peak in the estimated scatter coefficient μ_s has similar magnitude as the underestimation of the absorption coefficient μ_a in this region. Thus, this effect can probably be explained as extinction of the collimated transmittance that is erroneously considered by the model system to be scattering, while it is actually absorption. The lower accuracy of the estimated optical properties in the region of high absorbance by the water peak can therefore probably be related to the lower signal to noise ratio of the measurements in this region. It should

also be noted that the inputs to the inverse adding-doubling program (T_t & R_t) have been measured sequentially with a change and recalibration of the setup in between. This may have induced small deviations from the assumptions made in the modelling, which might not be observed in a double integrating sphere setup.

The satisfactory agreement between both curves brings us to the conclusion that the experimental setup with a single integrating sphere in combination with the inverse adding-doubling program with fixed anisotropy factor is useful for the estimation of optical properties. However, one should be aware that the absolute accuracy of the estimates is considerably lower in the regions of high absorption (by water).

B. Validation of the Experimental Setup for Variable Anisotropy Factor

The inverse adding-doubling program used in the previous section has been extended for simultaneous estimation of all three optical properties (μ_a, μ_s and g) by inclusion of the collimated transmittance T_c. The upper plot in Figure 3 shows the values for the absorption coefficient μ_a estimated by means of this extended program together with the values obtained from Mie theory (cfr. Fig. 2). The agreement between both curves is again very good. In this case, the absorption peak of water around 1450 nm has even been estimated quite accurately.

The middle plot of Figure 3 shows the values of the scattering coefficient μ_s estimated from the measurements by means of the extended inverse adding-doubling program together with the values obtained from Mie theory. It can be seen that the profile of the scattering coefficient with the increasing wavelength is highly similar, especially in the region from 600 to 1000 nm. For higher and lower wavelengths the extended inverse adding-doubling program gives lower scattering values than the Mie theory. From the inserted close-up it can be seen that there is no peak around 1450 nm as was the case for the inverse adding-doubling with fixed

anisotropy factor (Fig. 2), but the estimated scattering coefficients suddenly drop to 0.1 mm^{-1} around 1350 nm. This can probably be explained by the fact that the measured collimated transmittance values in this region were slightly higher than the ones obtained from the total transmittance measurement. This is not possible from a theoretical point of view and therefore brings the modelling system into trouble. If we compare Figures 2 and 3, it is hard to conclude which of both approaches gives the best estimates for the optical properties compared to Mie theory, because they both perform quite well and have become less reliable in the region above 1400 nm.

The lower plot in Figure 3 shows the values for the anisotropy factor g estimated from the measurements by means of the extended inverse adding-doubling approach together with the ones obtained from Mie theory. In the region from 450 to 900 nm there is good agreement between both curves. Above 900 nm the decrease with increasing wavelength is higher in the curve obtained by the inverse adding-doubling. Around 1350 nm a sudden drop in the estimated anisotropy factor can be observed in the curve for the inverse adding-doubling. This drop occurs at the same wavelength as the sudden drop in the scattering coefficient (middle plot in Fig. 3) and can be addressed to the same phenomenon of numerical instability due to violation of the assumptions, low signal to noise ratio and high correlation between the collimated and total transmittance in this region of low scattering and high absorbance. Therefore, it can be concluded that the estimates for the anisotropy factor are not very reliable in this region. However, it should be noted that the effect of this jump in the estimated anisotropy factor on the estimated values for the absorption and scattering coefficients is rather limited.

From the comparison of the absorption and scattering values obtained by both inverse adding-doubling approaches to the ones obtained by Mie theory it can be concluded that both are

nearly equally capable of giving useful estimates of the bulk optical absorption and scattering properties of the sample under study. Due to the high correlation between T_t and T_c the extended inverse adding-doubling approach with its three measurements for three unkowns does not necessarily give a unique solution for μ_s and g. This can be seen as clear jumps in the estimated anisotropy factor g which correspond to deviations in the estimated values for the scattering coefficient μ_s. Since these jumps in g are so clear, we can still use this approach, as long as we keep in mind that big jumps in g indicate regions of lower accuracy of the estimated values.

C. Apple Properties Estimated with Variable Anisotropy Factor

In Figure 4 the average bulk optical properties μ_a, μ_s and g estimated by means of the extended inverse adding-doubling program are shown for apple skin in the 350-2200 nm range for the three apple cultivars. The presented average curves were calculated from the 28 curves that have been estimated per cultivar (14 apples, 2 spots each) after removal of some obvious outliers (0, 2 and 3 for Royal Gala, Granny Smith and Braeburn, respectively). These obvious outliers are the result of the inversion algorithm ending up in a local minimum or becoming unstable. Thickness of the skin samples ranged from 0.11 to 0.54 mm.

In the NIR region the average absorption coefficient values μ_a are similar for all three cultivars and dominated by absorption peaks of water at 1450 and 1900 nm (Fig. 4 - top). In the visible region, the absorption coefficient values are, however, clearly different for the green Granny Smith apples with a sharp chlorophyll absorption peak at 675 nm compared to the yellow-red Royal Gala and Braeburn apples. Towards the ultraviolet region the absorption again increases considerably, due to water absorption.

The curves of the scattering coefficient values show that the apple skin is highly scattering, with values around 10-15 mm^{-1} (Fig 4 - middle). In the range 800-1800 nm, the scattering

coefficient μ_s decreases fairly smoothly with increasing wavelength. This corresponds to the general behaviour of the scattering characteristics of biological tissues [18]. Below 800 nm and above 1800 nm, the scattering coefficient, however, deviates from this monotonic decrease in the regions of the absorption bands of water and the pigments (e.g. chlorophyll). This deviation can be explained by the increase of the imaginary part of the complex refractive index of the scattering centers (i.e. skin cells), which leads to an increase in the scattering cross section [18].

The estimated spectra for the anisotropy coefficient g (Fig. 4 – bottom) show that apple skin is highly forward scattering with average values of 0.70, 0.63 and 0.67 for Royal Gala, Granny Smith and Braeburn apples, respectively. Although the spectra are fairly flat over the complete wavelength range, minima can be seen at the wavebands corresponding to the absorption peaks of water and the pigments. This can be explained by the fact that the increase in the imaginary part of the complex refractive index of the scattering centres at the absorption peaks causes a considerable decrease in the anisotropy factor g which is proportional to the absorption bands [18].

In Figure 5 the average bulk optical properties μ_a, μ_s and g estimated by means of the extended inverse adding-doubling program are shown for apple flesh in the 350-1900 nm range. The wavelength range has been reduced, because no reasonable estimates could be obtained beyond 1900 nm. This is a result of the very low amount of light in this region that is transmitted through the flesh samples with thickness ranging from 0.81 to 3.30 mm, due to the high absorption by water. No outliers were removed, so the presented curves are the average of 28 estimated curves per cultivar (14 apples, 2 spots each).

The average absorption coefficient values μ_a are again highly similar in the NIR region for all three cultivars and dominated by absorption peaks of water at 1450 and 1900 nm (Fig. 5 - top).

Moreover, the absorption coefficient values for the flesh are also highly similar in the visible region. This is in contrast to the observations for apple skin (Fig. 4 – top), where clear differences were observed between the green Granny Smith apples and the yellow-red Royal Gala and Braeburn apples. Towards the ultraviolet the absorption again increases considerably, due to water absorption.

The curves of the scattering coefficient values show that apple flesh tissue is considerably less scattering than apple skin tissue with values of 3-5 mm^{-1}. In the range 800-1800 nm, the scattering coefficient μ_s again decreases fairly smoothly with increasing wavelength. Below 800 nm the scattering coefficient of apple flesh also deviates from this monotonic decrease due to the increase in the imaginary part of the complex refractive index at absorption bands.

The estimated spectra for the anisotropy factor *g* (Fig. 5 – bottom) show that apple flesh is slightly less forward scattering than skin with average values of 0.66, 0.63 and 0.64 for Royal Gala, Granny Smith and Braeburn apples, respectively. The anisotropy factor spectra for apple flesh are a bit more undulating than for apple skin (Fig. 4 – bottom), but the minima corresponding to the absorption peaks of water and the pigments are a bit less clear.

D. Apple Properties Estimated with Fixed Anisotropy Factor

Figure 6 displays the average bulk optical properties μ_a and μ_s for apple skin in the 350-2200 nm range as estimated by means of the inverse adding-doubling program with fixed anisotropy factor. These values have been calculated based on the measured total transmittance and total reflectance values with the anisotropy factor *g* fixed at the average estimated values of 0.70, 0.63 and 0.67 for Royal Gala, Granny Smith and Braeburn apples, respectively. The presented average curves were again calculated from the 28 curves that have been estimated per cultivar (14 apples, 2 spots each) after removal of the obvious outliers. Although this procedure with

fixed anisotropy factor g was expected to be more stable than the one with variable g, more obvious outliers were observed (2, 14 and 2 for Royal Gala, Granny Smith and Braeburn, respectively). This can probably be explained by the fact that inclusion of the collimated transmittance adds an extra constraint which pulls the inversion out of local minima where it otherwise would get stuck.

The estimated average absorption coefficient values μ_a (Fig. 6 – top) show the same absorption features as the ones obtained from the inverse adding doubling with variable anisotropy factor (Fig. 4 – top). The scattering coefficient spectra estimated by this algorithm with fixed anisotropy factor confirm the fact that apple skin is highly scattering, with μ_s values above 10 mm^{-1} (Fig 6 - bottom). Below 600 nm and around 1450 and 1900 nm, the peaks in the scattering coefficient are, however, more pronounced compared to the ones obtained from the adding-doubling with variable g (Fig. 4 – middle). This can be explained as a result of fixing the scattering anisotropy g to one average value for all wavelengths. Since the anisotropy factor is fixed, the variations of the scattering cross section and the anisotropy factor due to changes in the complex refractive index of the scattering centres are both translated to changes in the scattering coefficient μ_s.

Figure 7 displays the average bulk optical properties μ_a and μ_s for apple flesh in the 350-1900 nm range as estimated by means of the inverse adding-doubling program with the anisotropy factor fixed at the average estimated values of 0.66, 0.63 and 0.64 for Royal Gala, Granny Smith and Braeburn apples, respectively. Similar to the case of the skin samples, more obvious outliers were observed for this algorithm with fixed anisotropy factor (2, 0 and 6 for Royal Gala, Granny Smith and Braeburn, respectively).

The estimated average absorption coefficient values μ_a are very similar to the ones obtained by means of the algorithm with variable *g* (Fig. 7 - top). The curves of the scattering coefficient values again show that the apple flesh is considerably less scattering than apple skin with values around 4 mm^{-1} (Fig. 7 – bottom). The curves are, however, less undulating than the ones observed for the algorithm with variable *g* (Fig. 5 – middle). The deviation at the water absorption bands of 1450 nm and 1900 nm from the monotonic decrease with increasing wavelength is here also more pronounced, due to the fixing of the anisotropy factor to an average value for all wavelengths.

E. Comparison of the inverse adding-doubling strategies

To be able to properly compare both inverse adding-doubling strategies (fixed and variable *g*) for the estimation of the bulk optical properties the estimated spectra are plotted on top of each other for both skin (Fig. 8) and flesh (Fig. 9) tissue. Since similar behaviour was observed for the different cultivars only the average spectra for the Royal Gala apples are plotted to avoid confusion due to overlapping curves. In case of the adding-doubling with variable anisotropy factor *g* there are two degrees of freedom for scattering: the scattering coefficient μ_s and the factor of anisotropy *g*. By fixing the latter, the other strategy only retains one degree of freedom which has to explain all variations in the light scattering by the sample: the scattering coefficient μ_s. Therefore, we will not compare the estimated values for the scattering coefficient μ_s, but those obtained for the transport scattering coefficient μ_s', which is calculated as:

$$\mu_s' = \mu_s(1-g) \qquad (1)$$

It can be seen from the plots that there is very good agreement between the spectra for the average bulk absorption coefficients μ_a (top figures) and transport scattering coefficients μ_s' (bottom figures) for apple skin (Fig. 8) and flesh (Fig. 9) tissue obtained with both strategies.

Apart from the average values we are also interested in the relative variation of the estimated optical properties around this mean throughout the spectrum. Therefore, the ratio of the standard deviation around the mean to the mean value of the optical properties is calculated at each wavelength for both strategies and for the three cultivars. These variation statistics are again calculated from the 28 curves that have been estimated per cultivar (14 apples, 2 spots each) after removal of the same obvious outliers. It should be noted that these relative variation statistics are not measures for the 'error' on the estimates, because the sample set is subjected to biological variation (different apples, different shelf-life, sunlit and shade side).

The wavelength dependent relative variation in the estimated optical properties for apple skin is displayed in Figure 10. Since similar behaviour was observed for the different cultivars only the average spectra for the Royal Gala apple samples are plotted to avoid confusion due to overlapping curves. It can be seen that the variation of the absorption coefficient μ_a is fairly constant around 20 % over the wavelength range from 1400 to 2200 nm (Fig. 10 – top). Below 1400 nm the relative variation increases with decreasing wavelength. For the region from 800 to 1400 nm this can probably be explained by the low absorption coefficient values in this region, which make that a small variation is considered high on a relative scale. In the visible range, the absorption values are, however, higher, such that these high relative variations probably say more about the biological variation in optical properties (e.g. different pigment concentrations at different ripeness stages). Similar behavior is observed for the absorption coefficient μ_a (Fig. 11 – top) profiles of apple flesh with constant variation around 20 % in the 1400-1900 nm range

and increasing relative variation with decreasing wavelength below 1400 nm. A maximum is reached in the 600-800 nm range, which is considerably higher for the Gala cultivar. It should also be noted that there a peak was observed in the relative variation of the estimated absorption coefficients μ_a for the Granny Smith and Braeburn cultivars around 675 nm. A possible explanation for these observations may be found in the fact that the Granny Smith and Braeburn apples were still in an early ripening stage at the beginning of the experiment, while the Gala apples were already in a further stage. The Granny Smith and Braeburn apples may therefore have had some active chlorophyll left in their flesh below the skin, which has become inactive due to further ripening during the three weeks storage at room temperature. This process might explain the peaks in the relative variation of μ_a at 675 nm. This hypothesis should, however, be investigated more in detail. This falls out of the scope of this paper, but will be the subject of a future study.

Inspection of the relative variation in the transport scattering coefficient μ_s' showed that the relative variation is fairly constant around 20 % for the Royal Gala (Fig. 10 – bottom) and Granny Smith apples, and around 25 % for the Braeburn apples over the entire wavelength range. Only in the UV-VIS region below 600 nm the relative variation increases up to 50 % with increasing wavelength. This fairly constant relative variation throughout the spectrum could have been expected from the physics of light scattering in biological tissues, where the scattering coefficient decreases monotonically with increasing wavelength as a function of the size and concentration of the scattering centres [18]. A change in this size and concentration of the scattering centres (due to biological variation or ripening) will thus result in an approximately constant relative change in the transport scattering coefficient. Similar behaviour

was observed for the estimated transport scattering coefficient μ_s' (Fig. 11 – bottom) profiles of flesh tissue.

For the relative variation in the scattering coefficient μ_s profiles of skin and flesh (Fig. 10 & 11 – middle) a similar behaviour can be observed as for the transport scattering coefficient μ_s' (Fig. 10 & 11 – bottom) in the range from 800 to 2200 nm. In the wavelength region below 800 nm, however, a considerable increase was observed in the relative variation for the scattering coefficients μ_s estimated for the Royal Gala and Braeburn cultivar by the inverse adding-doubling strategy with variable *g*. Since these effects are not observed in the transport scattering coefficient μ_s' spectra, they must have been counteracted by a simultaneous increase in the estimated anisotropy factor *g*. This means that the individual estimates of the scattering coefficient μ_s and the anisotropy factor *g* are less stable than the transport scattering coefficient μ_s', calculated from them. This behaviour can be interpreted as a form of exchangeability of the scattering information comprised in the scattering coefficient μ_s and the anisotropy factor *g*.

F. Discussion

Figure 12 shows the average bulk optical properties μ_a and μ_s' estimated by the inverse adding-doubling approach with variable *g* for skin and flesh tissue of Granny Smith apples in the 650-1000 nm range together with a reproduction of the values obtained by time resolved spectroscopy (TRS) on intact apples of this cultivar found in literature. The latter values have been extracted by visual inspection of Fig. 2 (μ_a) and Fig. 5 (μ_s') in reference [10].

As can be seen from the upper plot in Fig. 12, the shape of the absorption coefficient spectra obtained by time resolved spectroscopy on intact apples and for inverse adding-doubling

on apple flesh is very similar. They both show a small absorption peak of chlorophyll at 675 nm and one for water around 970 nm. The estimated values for apple flesh from the inverse adding-doubling are, however, offset by 0.03-0.04 mm^{-1}. The absorption coefficient curve of apple skin obtained by inverse adding-doubling has a similar water peak around 975 nm, but the chlorophyll peak at 675 nm is far higher, because of the high concentration of chlorophyll in the skin of Granny Smith apples. This strengthens the hypothesis made in [10] that the optical properties measured by TRS are dominated by the flesh properties. Apart from the similarities in shape the values estimated by inverse adding-doubling for skin tissue are even more offset (0.07 mm^{-1}) compared to the TRS values for intact apple. A possible explanation for these offsets can be found in the fact that the inverse adding-doubling does not account for light losses during the integrating sphere measurements. In this region of low absorption and high scattering, a portion of the incident light can leave the sample at the edges without being measured as either reflectance or transmittance. Since the 1D approximation of the radiative transport equation by adding-doubling does not account for these light losses, this portion will be considered as absorbed by the sample and thus contribute to the absorption coefficient [15]. Since this effect will be observed in all optical properties measured in this way and the shape of the absorption curve is retained, this is not a big issue when one is only interested in relative changes in the optical properties. However, when one needs the absolute values of the optical properties (e.g. for precise light transport simulations) this might cause dramatic errors. In that case an inversion method which takes these light losses into account, such as an inverse Monte Carlo approach, should be used.

The curves for the transport scattering coefficient μ_s' estimated by the inverse adding-doubling (IAD) for skin and flesh tissue and by TRS for intact apples (Fig. 12 – bottom) show a

similar monotonic decrease with increasing wavelength. The values obtained from TRS for intact apples are a 0.6-0.7 mm^{-1} higher and 2.3-2.4 mm^{-1} lower than the ones obtained by IAD for flesh and skin tissue, respectively. The fact that the values obtained from TRS are in between those for skin and flesh tissue, but closer to those for flesh tissue could have been expected, because the light that goes through an intact apple in a TRS measurement has to cross the apple skin twice, but travels the largest distance through the flesh.

4. Conclusions

The optical properties of apple skin and flesh tissue samples have been estimated in the 350-2200 nm range for three cultivars from single integrating sphere measurements by means of two inverse adding-doubling strategies: with fixed and variable anisotropy factor g. First, the experimental setup and both inversion strategies have been validated by comparing the optical properties estimated for a monodisperse polystyrene suspension with known particle size and concentration to the values obtained from Mie theory. From this comparison it was concluded that both strategies are nearly equally capable of giving useful estimates of the bulk optical absorption and scattering properties of the sample under study. Due to the high correlation between the total T_t and collimated transmittance T_c the extended inverse adding-doubling approach with its three measurements for three unknowns does, however, not necessarily give a unique separation of the scattering properties into the scattering coefficient μ_s and the anisotropy factor g.

These approaches have then been applied to the apple tissue measurements to estimate average values for the bulk optical properties of the samples from the different cultivars. The observed spectra for the absorption coefficient μ_a were dominated by absorption by water in the NIR (especially at 1450 and 1900 nm) and by pigments and chlorophyll (at 675 nm) in the

visible region. As expected, the latter was found to be much higher in skin tissue than in flesh tissue. From the spectra of the scattering coefficient μ_s was observed that apple tissue also follows the monotonic decrease with increasing wavelength that has been reported for other biological tissues. Apple skin tissue was, however, found to be about 3 times more scattering and slightly less forward scattering than the flesh tissue. Based on these observations it can be concluded that proper modelling of light transport through intact apples should be done with a model that considers at least two different bulk layers: skin and flesh.

Similar estimates for the average bulk absorption coefficient μ_a and transport scattering coefficients μ_s' were obtained with both adding-doubling strategies, but the inclusion of the extra measurement (T_c) in the strategy with variable g gave less obvious outliers, thanks to the extra constraint. Therefore, we suggest use of the strategy with variable anisotropy factor g when the anisotropy factor of the samples is not known a priori. Due to the exchangeability of the scattering information contained in the scattering coefficient μ_s and the anisotropy factor g, the scattering properties can, better be expressed in terms of the transport scattering μ_s', which was found to be a more stable estimate.

Finally, the estimates for the average absorption coefficient μ_a and transport scattering coefficient μ_s' obtained for Granny Smith apples were compared to the values from time resolved spectroscopy found in literature in the 650-1000 nm range. It was found that both techniques give similar absorption coefficient profiles, but that the inverse-adding doubling overestimates absorption by not correcting for the light losses in the setup. The values of the transport scattering coefficient μ_s' obtained from TRS are, as expected, in between those for skin and flesh tissue, but closer to those for flesh tissue. From this comparison to the values found it literature it can therefore be concluded that the applied approach with a single integrating sphere and inverse

adding-doubling is useful to obtain relative estimates of the optical properties. However, if precise absolute values of the absorption coefficient are needed, we suggest to use a modelling approach that takes the light losses into account (e.g. inverse Monte Carlo).

Acknowledgements

This research was performed at Newcastle University during a stay of Wouter Saeys as a visiting Postdoctoral Fellow funded by the Research Foundation – Flanders (FWO). Maria A. Velazco-Roa and Suresh N. Thennadil are both funded by the Engineering and Physical Sciences Research Council – UK (EPSRC) through grants GR/S50441/01 and GR/S50458/01.

References

1. B. M. Nicolaï, K. Beullens, E. Bobelyn, A. Peirs, W. Saeys, K. I. Theron, and J. Lammertyn, ”Nondestructive measurement of fruit and vegetable quality by means of NIR spectroscopy: A review”, Postharvest Biol. Technol., **46** (2), 99-118 (2007).
2. J. Lammertyn, B. Nicolaï, K. Ooms, V. De Smedt, and J. De Baerdemaeker, “Non-destructive measurement of acidity, soluble solid, and firmness of jonagold apples using NIR-spectroscopy”, Trans. Am. Soc. Agric. Eng. **41,** 1089-1094 (1998).
3. A. Peirs, A. Schenk, and B. M. Nicolaï, “Effect of natural variability among apples on the accuracy of VIS-NIR calibration models for optimal harvest date predictions”, Postharvest Biol. Technol. **35,** 1-13 (2005).
4. V. A. McGlone, P. J. Martinsen, C. J. Clark, and R. B. Jordan, “On-line detection of Brownheart in Braeburn apples using near infrared transmission measurements”, Postharvest Biol. Technol. **37**, 142-151 (2005).

5. B. Park; J. A. Abbott, K. J. Lee, C. H. Choi, and K. H. Choi, “Near-infrared diffuse reflectance for quantitative and qualitative measurement of soluble solids and firmness of Delicious and Gala apples”, Trans. Am. Soc. Agric. Eng. **46,** 1721-1731 (2003).
6. E. Mehinagic, G. Roayer, R. Symoneaux, D. Bertrand and F. Jourjon, “Prediction of the sensory quality of apples by physical measurements”, Postharvest Biol. Technol. **34,** 257-269 (2004).
7. Y. Liu, Y. Ying, H. Yu, and X. Fu, “Comparison of the HPLC method and FT-NIR analysis for quantification of glucose, fructose and sucrose in intact apple fruits”, J. Agric. Food Chem. **54,** 2810-2815 (2006).
8. J. Xing, W. Saeys, and J. De Baerdemaeker, “Combination of chemometric tools and image processing for bruise detection on apples”, Comput. Electron. Agric. **56,** 1-13 (2007).
9. M.L. Oey, E. Vanstreels, J. De Baerdemaeker, E. Tijskens, H. Ramon, M. Hertog, and B.M. Nicolaï, “Effect of turgor on micromechanical and structural properties of apple tissue: a quantitative analysis”, Postharvest Biol. Technol. **44** (3), 240-247 (2007).
10. R. Cubeddu, C. D’Andrea, A. Pifferi, P. Taroni, A. Torricelli, G. Valentini, C. Dover, D. Johnson, M. Ruiz-Altisent, and C. Valero, “Nondestructive quantification of chemical and physical properties of fruits by time-resolved reflectance spectroscopy in the wavelength range 650-1000 nm”, Appl. Opt. **40,** 538-543 (2001).
11. B. M. Nicolai, B. E. Verlinden, M. Desmet, S. Saevels, W. Saeys, , K. Theron, R. Cubeddu, A. Pifferi, and A. Torricelli, “Time-resolved and continuous wave NIR reflectance spectroscopy to predict soluble solids content and firmness of pear”, Postharvest Biol. Technol., **47** (1), 68-74 (2007).

12. D. G. Frazer, R. B. Jordan, R. Künnemeyer, V. A. McGlone, “Light distribution inside mandarin fruit during internal quality assessment by NIR spectroscopy”, Postharvest Biol. Technol. **27,** 185-196 (2003).
13. T. L. Troy, S. N. Thennadil, “Optical properties of human skin in the near infrared wavelength range of 1000 to 2200 nm”, J. Biomed. Opt. **6,** 167-176 (2001).
14. M.A. Velazco-Roa, and S.N. Thennadil, “Estimation of complex refractive index of polydisperse particulate systems from multiple-scattered ultraviolet-visible-near-infrared measurements”, Appl. Opt. **46**, 3730-3735 (2007).
15. S. A. Prahl, M. J. C. van Gemert, and A. J. Welch, “Determining the optical properties of turbid media by using the adding-doubling method”, Appl. Opt. **32**, 559-568 (1993).
16. G. de Vries, J. F. Beek, G. W. Lucassen, and M. J. C. van Gemert, “The Effect of Light Losses in Double Integrating Spheres on Optical Properties Estimation”, IEEE J. Quantum Electron. **5**, 944-947 (1999).
17. G. M. Hale, and M. R. Querry, “Optical constants of water in the 200-nm to 200-μm wavelength region”, Appl. Opt. **12**, 555-563 (1972).
18. A. N. Bashkatov, E. A. Genina, V. I. Kochubey, and V. V. Tuchin, “Optical properties of subcutaneous adipose tissue in the spectral range 400-2500 nm”, Opt. Spectrosc. **99**, 836-842 (2005).

Figure captions

Fig. 1. (Color online) Schematic representation of the different measurement configurations: a) Collimated transmittance measurement b) Total diffuse transmittance measurement c) Total diffuse reflectance measurement

Fig. 2. (Color online) Bulk optical properties μ_a (top) and μ_s (bottom) in the 450-1800 nm range for a monodisperse polystyrene suspension (diameter 0.45 μm and concentration 0.15% by weight of solids) in water estimated by means of Mie theory (circles) and by means of the inverse adding-doubling program with fixed g (stars).

Fig. 3. (Color online) Bulk optical properties μ_a (top), μ_s (middle) and g (bottom) in the 450-1800 nm range for a monodisperse polystyrene suspension (diameter 0.45 μm and concentration 0.15% by weight of solids) in water estimated by means of Mie theory (circles) and by means of the extended inverse adding-doubling program (stars).

Fig. 4. (Color online) Average bulk optical properties μ_a (top), μ_s (middle) and g (bottom) of apple skin in the 350-2200 nm range for the cultivars Royal Gala (solid line), Granny Smith (dashed line) and Braeburn (dotted line) estimated by means of the extended inverse adding-doubling program; The presented curves are the average of 28 estimated curves per cultivar (14 apples, 2 spots each).

Fig. 5. (Color online) Average bulk optical properties μ_a (top), μ_s (middle) and g (bottom) of apple flesh in the 350-1900 nm range for the cultivars Royal Gala (solid line), Granny Smith (dashed line) and Braeburn (dotted line) estimated by means of the extended inverse adding-doubling program; The presented curves are the average of 28 estimated curves per cultivar (14 apples, 2 spots each).

Fig. 6. (Color online) Average bulk optical properties μ_a (top), μ_s (bottom) of apple skin in the 350-2200 nm range for the cultivars Royal Gala (solid line), Granny Smith (dashed line) and Braeburn (dotted line) estimated by means of the inverse adding-doubling program with fixed anisotropy factors *g* of 0.70, 0.63 and 0.67, respectively; The presented curves are the average of 28 estimated curves per cultivar (14 apples, 2 spots each).

Fig. 7. (Color online) Average bulk optical properties μ_a (top), μ_s (bottom) of apple flesh in the 350-1900 nm range for the cultivars Royal Gala (solid line), Granny Smith (dashed line) and Braeburn (dotted line) estimated by means of the inverse adding-doubling program with fixed anisotropy factors *g* of 0.66, 0.63 and 0.64, respectively; The presented curves are the average of 28 estimated curves per cultivar (14 apples, 2 spots each).

Fig. 8. Average bulk optical properties μ_a (top), $\mu_{s'}$ (bottom) of apple skin in the 350-2200 nm range for the cultivars Royal Gala, Granny Smith and Braeburn estimated by means of the extended inverse adding-doubling program (solid lines) and the inverse adding-doubling program with fixed anisotropy factors (dashed lines) *g* of 0.70, 0.63 and 0.67, respectively; The presented curves are the average of 28 estimated curves per cultivar (14 apples, 2 spots each).

Fig. 9. Average bulk optical properties μ_a (top), $\mu_{s'}$ (bottom) of apple flesh in the 350-1900 nm range for the cultivars Royal Gala, Granny Smith and Braeburn estimated by means of the extended inverse adding-doubling program (solid lines) and the inverse adding-doubling program with fixed anisotropy factors (dashed lines) *g* of 0.66, 0.63 and 0.64, respectively; The presented curves are the average of 28 estimated curves per cultivar (14 apples, 2 spots each).

Fig. 10. Relative variation of the estimated bulk optical properties μ_a (top), μ_s (middle) and $\mu_{s'}$ (bottom) of apple skin in the 350-2200 nm range for the cultivars Royal Gala, Granny Smith and Braeburn estimated by means of the extended inverse adding-doubling program (solid lines) and

the inverse adding-doubling program with fixed anisotropy factors (dashed lines) g of 0.70, 0.63 and 0.67, respectively; The presented curves are calculated from 28 estimated curves per cultivar (14 apples, 2 spots each).

Fig. 11. Relative variation of the estimated bulk optical properties μ_a (top), μ_s (middle) and $\mu_{s'}$ (bottom) of apple flesh in the 350-1900 nm range for the cultivars Royal Gala, Granny Smith and Braeburn estimated by means of the extended inverse adding-doubling program (solid lines) and the inverse adding-doubling program with fixed anisotropy factors (dashed lines) g of 0.66, 0.63 and 0.64, respectively; The presented curves are calculated from 28 estimated curves per cultivar (14 apples, 2 spots each).

Fig. 12. Comparison of the average bulk optical properties μ_a (top) and $\mu_{s'}$ (bottom) in the 650 to 1000 nm range for skin (dashed line) and flesh (solid line) tissue of Granny Smith apples obtained by the inverse adding-doubling (IAD) approach to the values presented in [9] (stars) obtained by Time Resolved Spectroscopy (TRS) on intact apples.

Figures

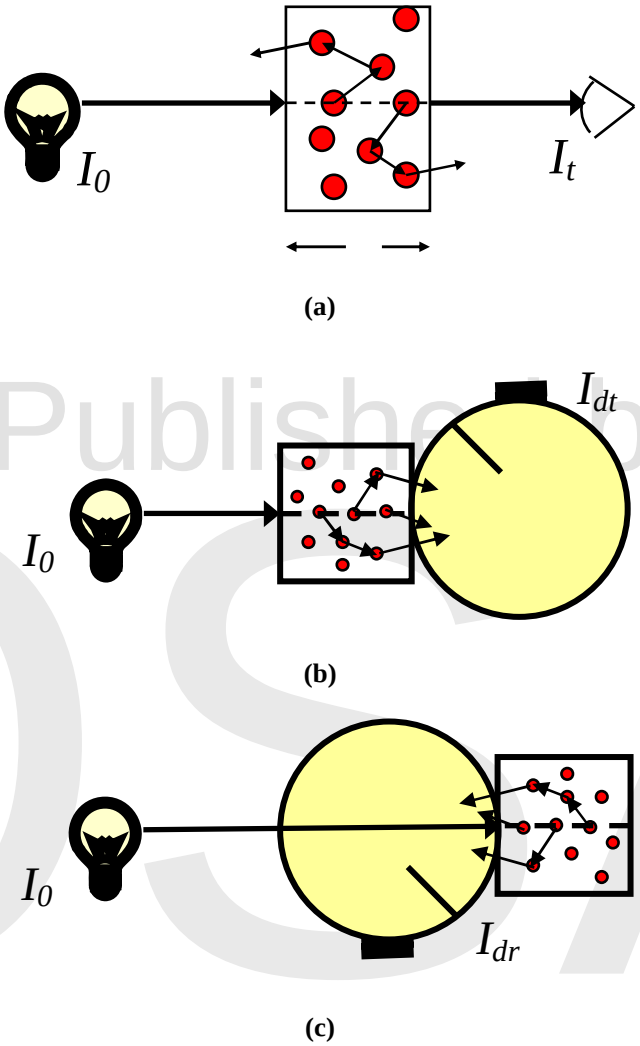

Fig. 1. (Color online) Schematic representation of the different measurement configurations: a) Collimated transmittance measurement b) Total diffuse transmittance measurement c) Total diffuse reflectance measurement

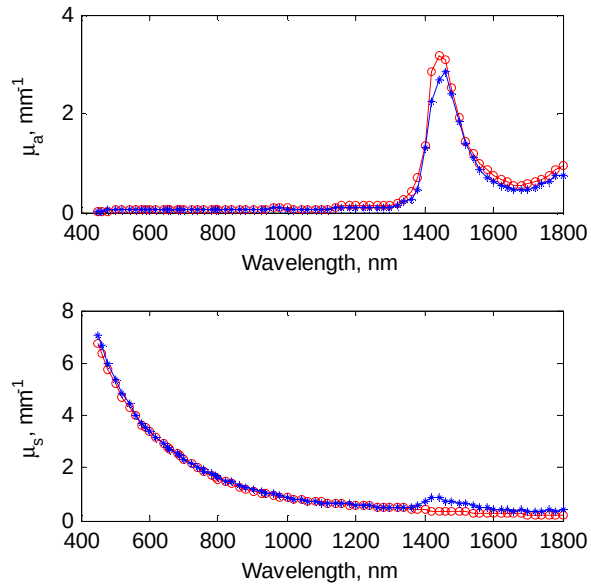

Fig. 2. (Color online) Bulk optical properties μ_a (top) and μ_s (bottom) in the 450-1800 nm range for a monodisperse polystyrene suspension (diameter 0.45 μm and concentration 0.15% by weight of solids) in water estimated by means of Mie theory (circles) and by means of the inverse adding-doubling program with fixed g (stars).

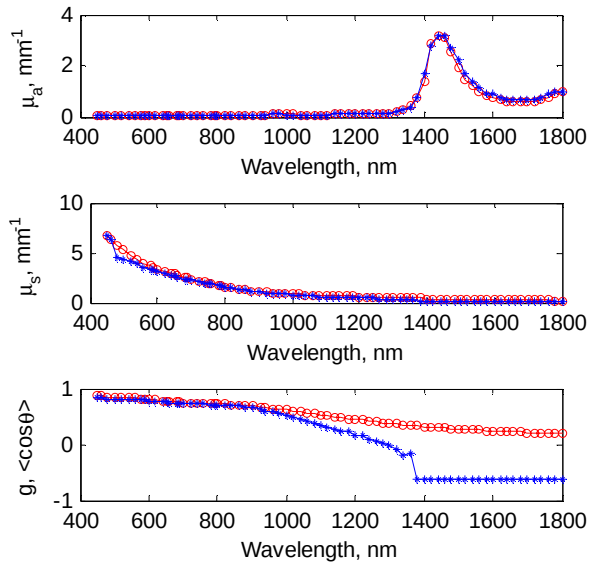

Fig. 3. (Color online) Bulk optical properties μ_a (top), μ_s (middle) and g (bottom) in the 450-1800 nm range for a monodisperse polystyrene suspension (diameter 0.45 μm and concentration 0.15% by weight of solids) in water estimated by means of Mie theory (circles) and by means of the extended inverse adding-doubling program (stars).

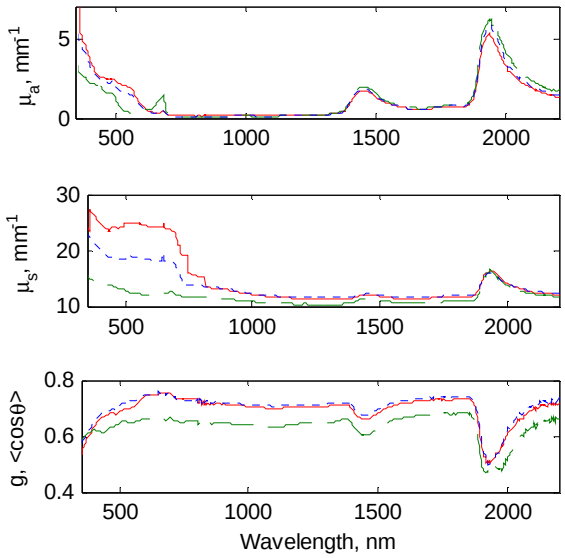

Fig. 4. (Color online) Average bulk optical properties μ_a (top), μ_s (middle) and g (bottom) of apple skin in the 350-2200 nm range for the cultivars Royal Gala (solid line), Granny Smith (dashed line) and Braeburn (dotted line) estimated by means of the extended inverse adding-doubling program; The presented curves are the average of 28 estimated curves per cultivar (14 apples, 2 spots each).

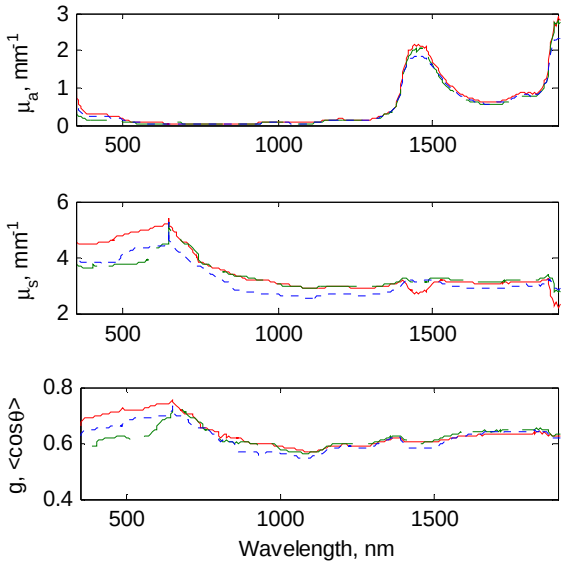

Fig. 5. (Color online) Average bulk optical properties μ_a (top), μ_s (middle) and g (bottom) of apple flesh in the 350-1900 nm range for the cultivars Royal Gala (solid line), Granny Smith (dashed line) and Braeburn (dotted line) estimated by means of the extended inverse adding-doubling program; The presented curves are the average of 28 estimated curves per cultivar (14 apples, 2 spots each).

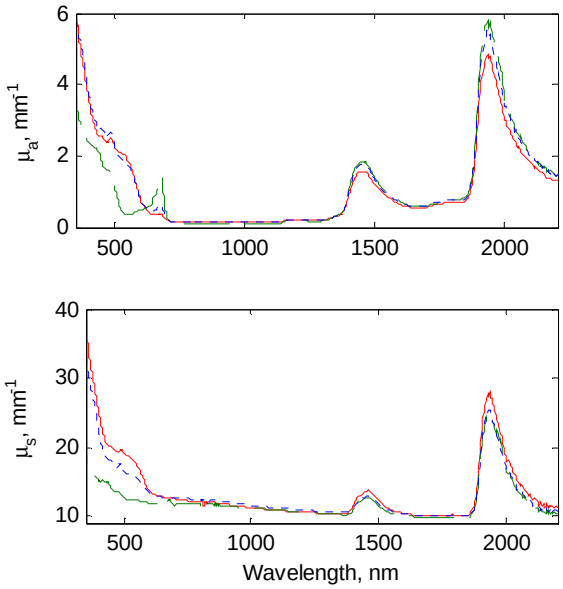

Fig. 6. (Color online) Average bulk optical properties μ_a (top), μ_s (bottom) of apple skin in the 350-2200 nm range for the cultivars Royal Gala (solid line), Granny Smith (dashed line) and Braeburn (dotted line) estimated by means of the inverse adding-doubling program with fixed anisotropy factors *g* of 0.70, 0.63 and 0.67, respectively; The presented curves are the average of 28 estimated curves per cultivar (14 apples, 2 spots each).

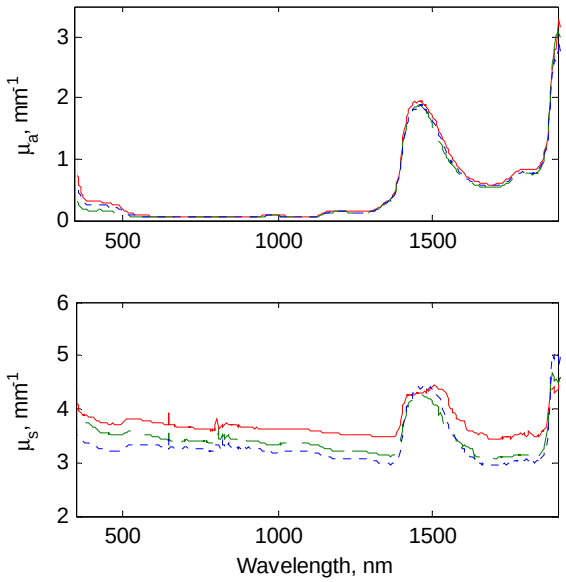

Fig. 7. (Color online) Average bulk optical properties μ_a (top), μ_s (bottom) of apple flesh in the 350-1900 nm range for the cultivars Royal Gala (solid line), Granny Smith (dashed line) and Braeburn (dotted line) estimated by means of the inverse adding-doubling program with fixed anisotropy factors g of 0.66, 0.63 and 0.64, respectively; The presented curves are the average of 28 estimated curves per cultivar (14 apples, 2 spots each).

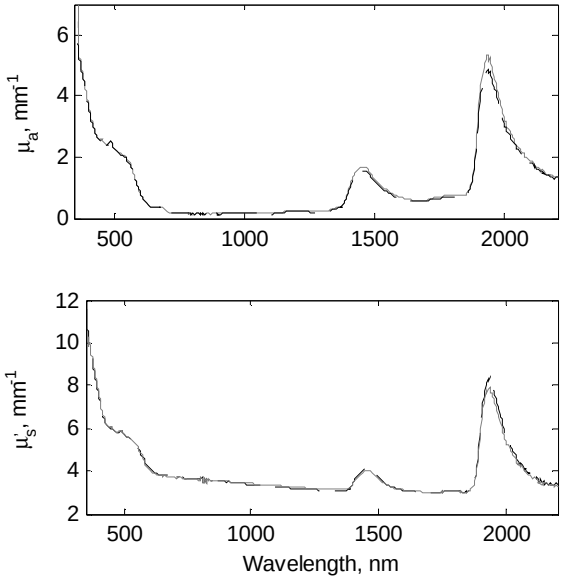

Fig. 8. Average bulk optical properties μ_a (top), $\mu_{s'}$ (bottom) of apple skin in the 350-2200 nm range for the Royal Gala apple samples estimated by means of the extended inverse adding-doubling program (solid lines) and the inverse adding-doubling program with a fixed anisotropy factor (dashed lines) *g* of 0.70; The presented curves are the average of 28 estimated (14 apples, 2 spots each).

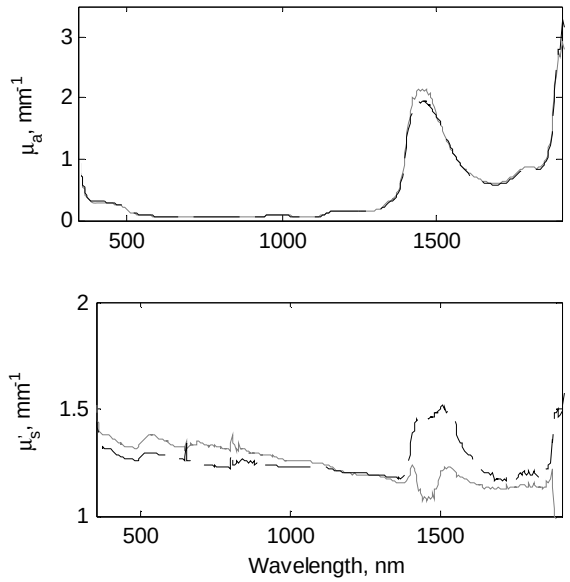

Fig. 9. Average bulk optical properties μ_a (top), $\mu_{s'}$ (bottom) of apple flesh in the 350-1900 nm range for the Royal Gala apple samples estimated by means of the extended inverse adding-doubling program (solid lines) and the inverse adding-doubling program with a fixed anisotropy factor (dashed lines) *g* of 0.66; The presented curves are the average of 28 estimated curves (14 apples, 2 spots each).

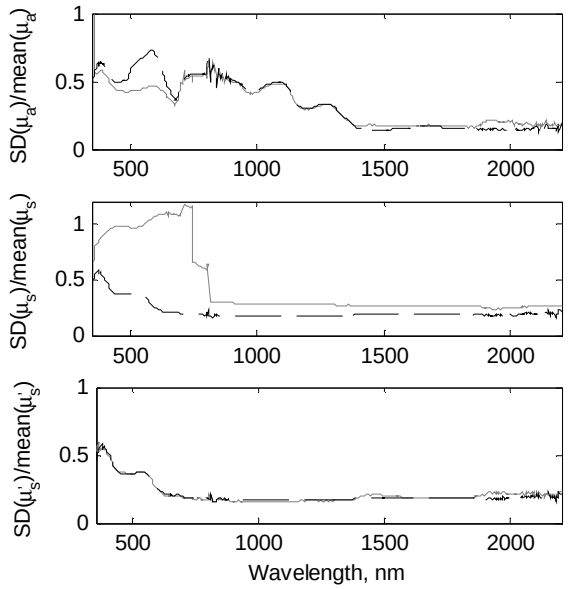

Fig. 10. Relative variation of the estimated bulk optical properties μ_a (top), μ_s (middle) and $\mu_{s'}$ (bottom) of apple skin in the 350-2200 nm range for the Royal Gala apple samples estimated by means of the extended inverse adding-doubling program (solid lines) and the inverse adding-doubling program with a fixed anisotropy factor (dashed lines) *g* of 0.70; The presented curves are calculated from 28 estimated curves (14 apples, 2 spots each).

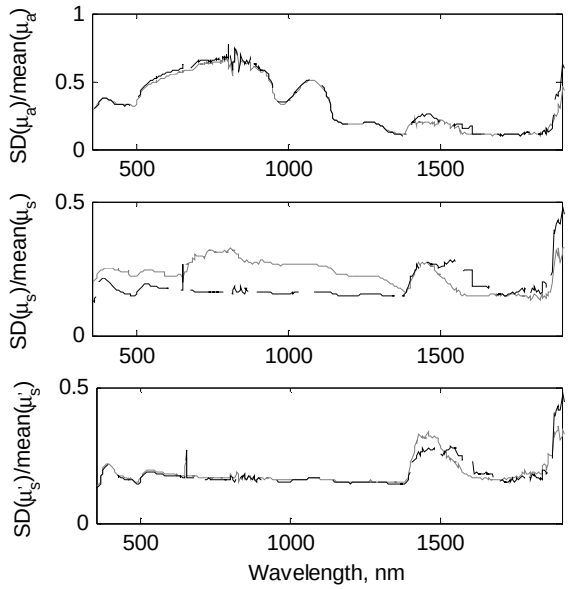

Fig. 11. Relative variation of the estimated bulk optical properties μ_a (top), μ_s (middle) and $\mu_{s'}$ (bottom) of apple flesh in the 350-1900 nm range for the Royal Gala apple samples estimated by means of the extended inverse adding-doubling program (solid lines) and the inverse adding-doubling program with a fixed anisotropy factor (dashed lines) *g* of 0.66; The presented curves are calculated from 28 estimated curves (14 apples, 2 spots each).

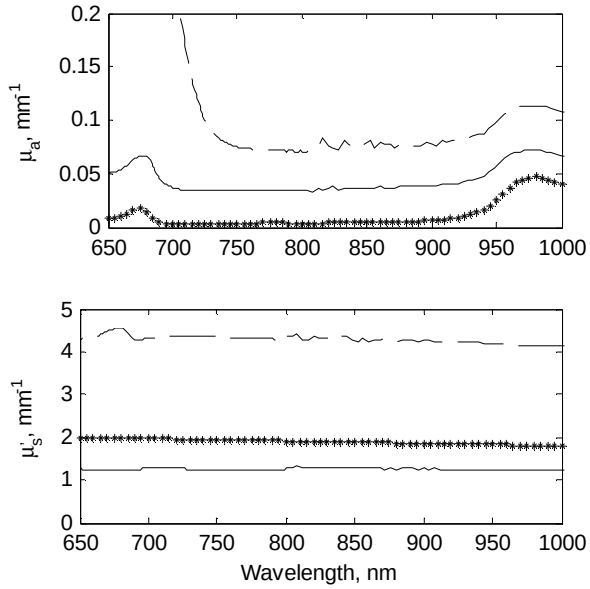

Fig. 12. Comparison of the average bulk optical properties μ_a (top) and $\mu_{s'}$ (bottom) in the 650 to 1000 nm range for skin (dashed line) and flesh (solid line) tissue of Granny Smith apples obtained by the inverse adding-doubling (IAD) approach to the values presented in [10] (stars) obtained by Time Resolved Spectroscopy (TRS) on intact apples.